Medicon Engineering Themes
Volume 7 Issue 4 October 2024
Article Type: Research Article
ISSN: 2834-7218

A Computational Study on Performance Analysis of Different Types of Tandem Solar Cells

Bibhuti Bhusan Nayak* and Tardup Lepcha

Mechanical Engineering Department, National Institute of Technology Sikkim, India

***Corresponding Author:** Bibhuti Bhusan Nayak, National Institute of Technology Sikkim, Department of Mechanical Engineering, Ravangla, Sikkim, India.

Received: September 28, 2024; **Published:** October 16, 2024

DOI: 10.55162/MCET.07.237

Abstract

The operating temperature of photovoltaic cells is an important parameter that influences their conversion efficiency. High operating temperatures greatly determine the maximum output power for the same conditions of solar radiation. In this paper a numerical approach have been conducted on a tandem solar cell of area 50x50 mm^2 so as to analyse the temperature variation of a solar cell kept in a tandem. This paper includes three tandem solar cells with different combinations of the top cell and bottom cell. A detailed study of thermal analysis on various type of tandem solar cells is carried out in the hilly regions. The tandem solar cells considered are mono- crystalline silicon-$MAPbI_3$ tandem, mono-crystalline silicon-$MAPbBr_3$ tandem and $MAPbI_3$ - $MAPbBr_3$ tandem. The trend in temperature variation with time is witnessed wherein the temperature difference between the top cell and bottom cell is also observed. The efficiency of the cells are calculated individually and the efficiency of the tandem is also calculated. The thermo physical property values used in the paper like thermal conductivity, specific heat capacity and density were collected and chosen from different papers mentioned in the reference. All the calculation's data that is the temperature, input power and the efficiency of tandem solar cell is with respect to the solar irradiation for the coordinate 88.6138 °E, 27.3314 °N GMT +5:30. The solar power and efficiency for different tandem cells has been compared for the whole day starting from 10 AM to 5 PM for a week. From the study the maximum power conversion efficiency obtained for $MAPbI_3$ - $MAPbBr_3$ tandem is 43.78% and minimum for silicon-$MAPbI_3$ tandem is 35.25%. The average power obtained highest for $MAPbI_3$ - $MAPbBr_3$ is 55.79W and lowest for silicon-$MAPbI_3$ tandem is 45.08W. The solar flux intensity is gradually increases and then decreases from 10 AM to 5 PM, the peak value of 908 W/m^2 is obtained at 11 AM of the day.

Keywords: Mono-crystalline silicon-$MAPbI_3$ tandem; silicon-$MAPbBr_3$ tandem; $MAPbI_3$ - $MAPbBr_3$ tandem solar cells; Power conversion efficiency; thermal analysis; simulation

Introduction

Solar energy is generally employed as electricity generating energy source in our modern world, hence solar energy is converted to electrical energy using solar cells, also known as solar panels. Solar cell is a device that uses the photovoltaic effect, which is a physical and chemical phenomenon, to transform light directly into electricity.

The solar cell plays vital role in energy conversion of light to electricity hence making it useful in many modern solar technologies. The modern solar cell is primarily made of silicon compounds. The solar cells are roughly divided into three generations namely the first generation, second generation and third generation.

The first generation solar cells includes inorganic wafer based solar cells like mono-crystalline and poly- crystalline silicon solar cells they have high conversion efficiency about 24-26%. The second generation includes the solar cells that are inorganic thin film based like CdTe and CIGS they have conversion efficiency of about 22%. These two generations of solar cells have higher efficiency but the cost of manufacturing is also high. The organic thin film based solar cell which have lower energy conversion efficiency of about 12-13% but have lower mafacturing cost makes the third generation solar cells.

In recent times the developement of organic-inorganic hybrid perovskite have emergred in solar cell technology. They inculcate in them high efficiency as well as low production cost. They have energy conversion efficiency of about 22%. Making them idle for mass usage unlike other new technology.

The energy conversion efficiency is the major concern for solar cells as the efficiency of a solar cells are affected directly by many factors like temperature, weather, type of material etc. The energy conversion efficiency of regular solar cells in practical case is about 13-17%. Researchers around the world are indulging themselves into researching about the improvement of efficiency. Regardless of how the technoogy is developed the solar cell with single junction can only have or achieve efficiency of about <30%. This is due to the Shockley-Queisser efficiency limit. The conversion efficiency of about 30% is not desirable in the long run and so this limit has to be surpassed.

The most reliable and promising answer to how do we surpass the S-Q limit is the multi-junction solar cells or tandem solar cells. It is a device where the absorbers with different bandgaps (E_g) are stacked one above the other to form a tandem and hence the name. With this arrangement the higher energy are absorbed by large bandgap kept at the front or top sub cells and the unabsorbed small energies are absorbed by the smaller bandgap subcells. The multiple p-n junctions are electrically connected via tunnel junctions or a shared electrode, resulting in a series electrical connection. There are several types of tandem solar cells depending on the manufacturing process and interconnection scheme used.

Until recently, attempts to produce tandem solar cells, aside from thin film silicon and III-V materials, had met with minimal success. Achieving effective high-band gap top cells and treatment incompatibilities such as junction degradation owing to high temperature procedures or other operations such as sputtering damage have been the two key hurdles for tandem sun cells. Perovskite photovoltaic, which have achieved the highest efficiency gains in history, with band gaps exceeding 1.5 eV, have opened up a slew of new possibilities for monolithic tandem solar cells. They're perfect for constructing optical and current matching since they may be deposited in either p-n or n-p sequence and have a readily tuneable band gap within the 1.48-2.3 eV range. Because of the low processing temperature, they may be employed in monolithic tandems with temperature- sensitive chalcogenide bottom cells like CZTSSe and CIGSSe, as well as in perovskite-silicon tandems.

Perovskite is a mineral, composed of calcium, titanium, oxygen in the form $CaTiO_3$. First time found in the Ural Mountains by Lev Perovski. Perovskite structure is called everything with the same ABX_3 generic form. The inclusion of perovskite in the solar energy was from late 00's but Si was always in solar cell technology. The improvement in the efficiency of Si has been gradual but the efficiency improvement for perovskite has been exponential. In just few years the efficiency has reached from mere 4% to 22%.

The stability of perovskite photovoltaic systems in high temperature and humidity is a critical hurdle for their development. With the replacement of formamidinium and the introduction of a mixture of formamidinium and caesium, some advancement toward thermal stability has been made. The large band gap formamidinium bromide absorber was combined with enhanced hole-transporting materials based on fluorene-dithiophene derivatives to obtain a remarkable V_{oc} of 1.47 V. A rising number of researches are looking at the stability of perovskite surfaces in real-world applications. The use of Al_2O_3 nanoparticles or chromium diffusion barriers was used to combat metal-migration-induced deterioration. Other reports say that changing the rest of the device layers increased the gadget's stability to ambient circumstances. It remains to be seen whether any of the offered alternatives can generate a device that is reliable enough for practical use. The growth of the TCE on top of a device that already has a perovskite layer is a common issue for perovskite tandems. Standard sputtering methods generate thermal and plasma damage, which must be handled.

The stability of the perovskite is not the only challenge faced by the perovskite used for the solar cell but also the problem of lead poisoning. As lead is vital for the perovskite; research is going on in this field to find an alternative for lead.

Todorov et al. [1] investigated the many sorts of tandem configurations as well as the perovskite, a recently introduced material in the solar energy business. In their paper "A road towards 25% efficiency and beyond: perovskite tandem solar cells. Perovskite solar cells have been a popular companion in tandem device architectures because to its unique mix of high efficiency, tuneable band gap, and gentle processing temperature, according to their research. Significant progress has been made with both monolithic and stacked device topologies in just a few years, with the latter already exceeding 25% efficiency. The invention of non-destructive TCE and CRL creation procedures to protect the delicate perovskite device structure has been a crucial reason in this accomplishment. While some attempts have been done to address long-term device stability, this is still a crucial issue for the large-scale implementation of perovskite solar cells in general and will determine their future.

Popovicia et al. [2] looked at the use of heat sinks and given a computer model to analyse the situation. In their report "Efficiency improvement of photovoltaic panels by using air cooled heat sinks" they determined in their article that the operating temperature of a solar panel has a significant impact on its conversion efficiency. The primary characteristics of the PV panels, the intensity of a voltage and current of the photovoltaic panel, which are presented globally as maximum output power, are the best way to investigate this impact. If no ribs are employed and the highest output power is 86 percent of the nominal one, the operating temperature of the PV panel hits around 56 °C in the examined situation. Even for small rib heights, the median temperature of the PV panel decreases when a heat sink is used. Simulations show that the temperature is decreased by at least 10 degrees Celsius compared to the baseline situation. This factor favours conversion efficiency, resulting in a maximum power output of more than 90% of the nominal value. The maximum power generated by a solar panel increases from 6.97 percent to 7.55 percent in the examined arrangement, compared to the basic scenario, for rib angles of 90° and 45°, respectively. Given the inherent need to ventilate double-skin facades during the summer, the proposed approach for cooling solar panels might be a low-cost, energy-efficient alternative. In order to authenticate these results, an experimental exploration will be realized in future works.

Anwer Askari et al. [3] investigated a two-junction tandem solar cell with c-Si and perovskite as absorption layers. In their paper "Performance Analysis of Perovskite on Si Tandem Solar Cell" The performance of a 2- terminal Perovskite/Si tandem solar cell was investigated in this research by altering physical and device factors. Some of the best feasible designs for improving the device's efficiency have also been presented. The intensity of incident light on the bottom cell after absorption by the top perovskite layer was calculated using the transfer matrix technique. This research looked at the generation of excitation rather than free carrier in an organic substance when light is incident. The results demonstrate that the overall efficiency of the structure is highly dependent on the thickness of the top perovskite layer, with a maximum power conversion efficiency (PCE) of 27 percent attained for a perovskite layer thickness of 170 nm.

Mitroi et al. [4] conducted a complete numerical simulation of tandem solar cell performance optimization employing c-Si and Cu_2O sub cells. The solar cell's single-diode model is used to run a numerical simulation. Both the model parameters and the parameters of the sub cells and tandem are determined using the numerical technique. The maximum output power is used to determine the thickness of the active layers c-Si and Cu_2O in tandem cells. For 0.64 m Cu_2O layer thickness and 60.62 m c-Si layer thicknesses, the tandem power conversion efficiency reaches 31.23 percent. When compared to individual cells, these thicknesses are greatly decreased, and the efficiency is equal to the theoretical limit at 298 K. Optical losses for each layer of the tandem, as well as a lower than unity injection efficiency in the active layers, will be included in a realistic model of the tandem. As a result, a lower tandem efficiency value is projected. Temperature is a role in diminishing tandem conversion efficiency, according to the numerical simulation; consequently, temperature should be considered in tandem cell design. The findings of this study provide guidance for the design and performance optimization of genuine tandem solar cells made up of Cu_2O and c-Si sub cells.

Mourshed et al. [5] published a study of maximum utilization of solar energy in the area by integrating many parts along with the solar panel in their paper "Experimental investigation and CFD analysis of a solar hybrid PV/T system for the sustainable development

of the rural northern part of Bangladesh." According to them, an effort was made to use solar energy more efficiently by designing a single pass hybrid photovoltaic thermal system under Bangladesh's climatic conditions. Because the photovoltaic module's electric energy conversion efficiency decreases as the ambient temperature rises, air or water is utilized to keep it cool. To achieve optimal utilization of solar energy, air was employed as the cooling medium for the solar panel, and a circular copper tube was put atop the glass collector for water heating. Furthermore, the energy generated by the solar panels was used to circulate the air, making the system self-sufficient. With a mass flow rate of 0.00158 and 0.00221 kg/s for water and air, respectively, at a solar radiation of 1050 W/m^2, maximum collector efficiency was found to be 24.64 percent for water and 11.20 percent for air. Furthermore, the hybrid system's combined efficiency was at 39.68 percent. The combined efficiency of glycerin and water at a 50:1 (percent of weight) ratio was up to 45.76 percent. The developed system's computational fluid dynamics (CFD) simulation and economic analysis substantially indicate the solar hybrid photovoltaic thermal system's potential as a future sustainable energy source.

From the literature it is found that there is limited study on performance comparison of all the solar tandem cells accommodated in the hilly regions. In this type of regions harvesting solar energy is quite challenging for the researchers.

Materials and Methods

Model Design

Geometry Description

A study of variation of temperature with time is done on tandem solar cell. The trend in the temperature distribution of two sub cells are recorded with changing time; starting from 10:00 AM to 5:00 PM on hourly basis. The maximum and minimum temperature at each hour is noted and presented in the tables.

A tandem solar cell of area 50 x 50 mm^2 is considered. The dimension of the tandem solar cell is generated after referring to various similar research paper. The area of all the tandem solar cell is same i.e 50x50 mm^2.

The geometry of tandem solar cells were constructed using ANSYS Space-Claim Software & Design Modeller. The geometry can also be imported from other external software like the Solid Works & Auto CAD. The geometry of the solar cell had to be kept as simple as possible for better result.

In total three combinations of tandem namely mono crystalline Si-$MAPbI_3$, mono crystalline Si-$MAPbBr_3$ and $MAPbI_3$-$MAPbBr_3$ (perovskite-perovskite) have been simulated. The mono crystalline Si has been used as the bottom layer in both the cases. In case of the perovskite-perovskite arrangement the top sub cell is $MAPbBr_3$ and the bottom sub cell is $MAPbI_3$.

To make a multi-junction device, there are three main approaches to combine silicon with other solar cells: two- terminal, mechanically stacked four-terminal, and optical coupling four-terminal. The sub-cells in two-terminal arrangements are connected in series by semiconductor material that transfers carriers from one sub cell to the other. The tandem device simply has two terminals and may be used as a regular single junction solar cell, making its integration into a PV module and system much easier. The necessity of current-match, however, limits the possibilities of materials in terms of band gaps because the sub cells are connected in series. The mechanical stacked four-terminal tandem device is the second arrangement, in which the sub cells are vertically stacked but each has its own terminals that can be controlled independently to their maximum power points. This technique eliminates the need for current-matching and a conductive layer between sub cells as compared to the two- terminal tandem setup. When scaled to module-sized regions, however, it is projected to have higher module and balance-of-systems costs, as well as increased power losses. An optical spectrum splitter is used in the third coupling setup to direct the optimum sections of the solar spectrum to each sub cell. The sub cells are operated independently of one another, allowing for greater flexibility in sub-cell selection. The problem of cell integration is transferred to the PV module designers in this configuration. However, spectrum filters are still relatively expensive at the moment.

When it comes to tandem solar cell design, the band gap selection is critical for high-performance devices. A bottom cell with a small band gap paired with a top cell with a big band gap is best for achieving efficiency greater than the S-Q limit under one-sun illumination

in a two-junction setup.

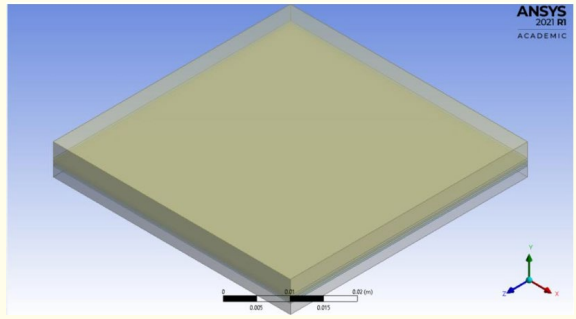

Figure 1: Geometry of the tandem solar cell.

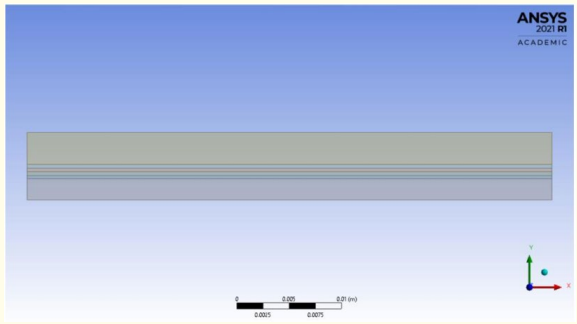

Figure 2: Different layers of tandem solar cells.

Though the thickness of the various layer are different while making the geometry the layer's thickness were altered as required for meshing. Area of the cell is same; the thickness is of varying unit as:

For tandem composed of Si-$MAPbI_3$:

t1 - 0.9 mm.

For tandem composed of Si-$MAPbBr_3$:

t2 - 0.9 mm.

For tandem composed of $MAPbI_3$-$MAPbBr_3$:

t3 - 0.9 mm.

The thickness of the individual layer is taken as:

Materials	*Tandem Solar Cell 1*	*Tandem Solar Cell 2*	*Tandem Solar Cell 3*
Glass	0.3	0.3	0.3
SnO_2	0.2	0.1	0.1
Rear Contact	0.2	0.3	0.3
Pv-Cell	0.1	0.1	-
$MAPbI_3$	0.1	-	0.1
$MAPbBr_3$	-	0.1	0.1

Table 1: Thickness of various layer of tandem solar cells in mm.

Some of the layers described in the table 1; describing materials property were not included in the geometry because their thickness are very small. The grid size of the mesh is taken as 0.0002 m; the mesh contained approximately 300000 numbers of elements.

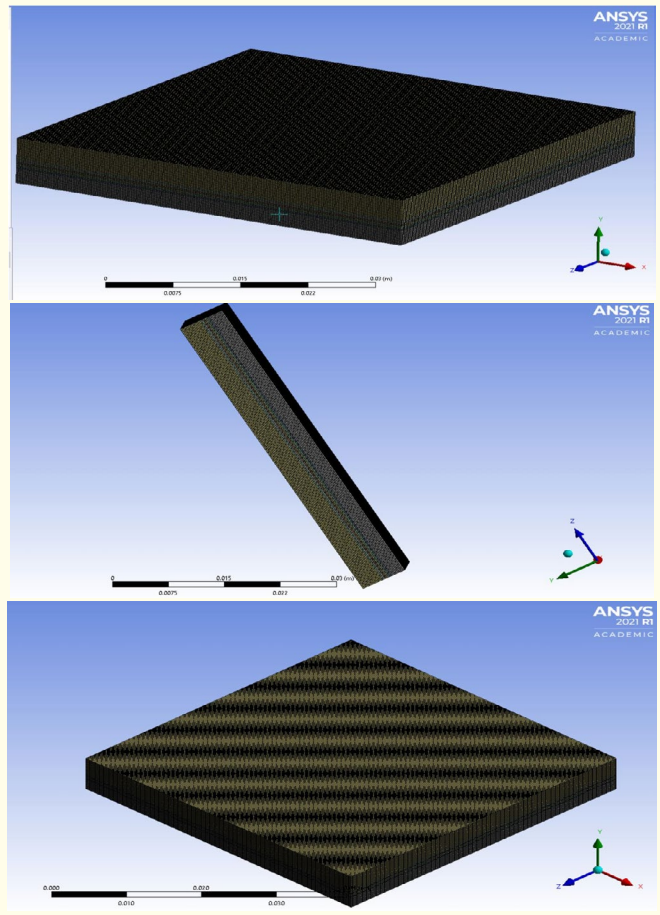

Figure 3: Meshed geometry of tandem solar cells.

Governing Equations

The numerical analysis is performed using ANSYS FLUENT Software as the solver. Computational fluid dynamics governing equation are used to investigate the interactive motion of large number of individual particles inside the fluid domain. This defines the various

parameters e.g. velocity, pressure, temperature at individual point inside fluid domain. The principle governing equation is as follows:

Continuity equation

$$\frac{du}{dx}+\frac{dv}{dy}+\frac{dw}{dz}=0$$

Momentum Equation

$$u\frac{dv}{dx}+v\frac{dv}{dy}+w\frac{dv}{dz}=-\frac{1}{p}\frac{dp}{dy}+v\left(\frac{d^2v}{dx^2}+\frac{d^2v}{dy^2}+\frac{d^2v}{dz^2}\right)$$

$$u\frac{dw}{dx}+v\frac{dw}{dy}+w\frac{dw}{dz}=-\frac{1}{p}\frac{dp}{dz}+w\left(\frac{d^2w}{dx^2}+\frac{d^2w}{dy^2}+\frac{d^2w}{dz^2}\right)$$

Energy equation

$$u\frac{dt}{dx}+v\frac{dt}{dy}+w\frac{dt}{dz}=\alpha\left(\frac{d^2t}{dx^2}+\frac{d^2t}{dy^2}+\frac{d^2t}{dz^2}\right)$$

The turbulence model used was the standard k-ϵ model. It's the foremost common turbulence model in CFD simulation, and k is that the turbulent and ϵ is that the dissipation rate of turbulent energy. This model is predicated on the time-averaged Naiver-Stokes equation, which assumes that the time-varying velocities of turbulence may be divided into time-averaged velocities and velocity-dependent velocities. Therefore, within the CFD evaluation for the study, air flow analysis was performed using the quality k-ϵ turbulence model because the analysis isn't complicated and its accuracy is nice in terms of computational convergence.

The model used to simulate the solar radiation is the specialized tool Solar Ray Tracing from Fluent software, value such as direct solar irradiance and diffused solar irradiance are required but alternatively solar calculator can also be used for required value of irradiance and diffused solar irradiation. It is with the help of solar calculator that simulation of the weather condition of Gangtok was done. The condition of weather simulated was fair weather out of the two options of which the other option was theoretical maximum. The mesh orientation was kept as 1, 0, 0 north and 0, 0, 1 east. The value of solar irradiation is calculated by using the pre-defined algorithm.

In a perovskite absorber, light exposure produces electron-hole pairs that use thermal energy to separate into free electrons and holes. The electrons move towards the electron transport layer (ETL) and the holes move towards the hole transport layer (HTL) as a result of the concentration gradient and an inherent electric field. Diffusion generated by concentration gradients and electrical drift forces control the transport of these charge carriers.

Global Positioning			
	Latitude	***Longitude***	***Time Zone***
Tandem Solar Cell 1	27.3314 N	88.6138 E	+5:30
Tandem Solar Cell 2	27.3314 N	88.6138 E	+5:30
Tandem Solar Cell 3	27.3314 N	88.6138 E	+5:30

Table 2: Global Positioning of tandem solar cell for simulation.

In Gangtok, the average wind speed is 1.4 m/s, with a maximum wind speed of roughly 7 m/s. The average temperature is 10.6°C, with temperatures ranging from -5.6°C to 22.8°C. The average relative humidity is roughly 87 percent, with a range of 33 to 100 percent. The wind rose in Gangtok indicates that the wind is primarily from the south, accounting for 19.77 percent of all wind directions.

As a worldwide absorption coefficient of solar radiation, a=0.7 [16], the optical characteristics of a solar cell were constructed. The outside surface of the solar panel was subjected to low convective heat transfer, with a heat transfer coefficient of hconv = 8 $W/m^2.K$ [16].

The surface to surface radiation model was applied. The radiation transmission in an enclosure of gray- diffuse surfaces may be accounted for using the surface-to-surface radiation model. The energy transfer between two surfaces is influenced by their size, separation distance, and direction, among other factors. A geometric function known as a "view factor" accounts for these characteristics.

The primary assumption of the S2S model is that any absorption, emission, or scattering of radiation can be ignored; therefore, only "surface-to-surface'' radiation needs to be considered for analysis.

The S2S radiation model is computationally very expensive when there is a large number of radiating surfaces. To reduce the computational time as well as the storage requirement, the number of radiating surfaces is reduced by creating surface "clusters''. The surface clusters are made by starting from a face and adding its neighbours and their neighbours until a specified number of faces per surface cluster is collected. An algorithm has been implemented for the creation of surface clusters which is faster and supports non- conformal interfaces, hanging nodes, or mesh adaption. This algorithm is now the default. If you wish to use the old algorithm, you may use the TUI command but adaption and non-conformal interfaces will not be supported.

The radiosity is calculated for the surface clusters. These values are then distributed to the faces in the clusters to calculate the wall temperatures. Since the radiation source terms are highly non-linear (proportional to the fourth power of temperature), care must be taken to calculate the average temperature of the surface clusters and distribute the flux and source terms appropriately among the faces forming the clusters.

The property described in table 3; are all taken from various sources as the properties like thermal conductivity, density and specific heat capacity are already available for these materials and no calculation is needed for them. The thermo physical properties of the two perovskites were taken from [17]. Some of the commonly used materials are predefined in the Fluent. The materials described in the table 3 are all used in solar panels used in practical life except for the two perovskite whose use are not so popular as of now. These materials are only limited to lab experiments due to various problems faced by the material in the practical environment among which temperature is one factor. The rear contact is made of aluminium whose properties are readily available in numerous sources.

Sl. No.	*Name of the Material*	*Density (Kg/m^3)*	*Thermal Conductivity (W/m K)*	*Specific Heat (J/ Kg K)*
1	Glass	3000	1.8	500
2	SnO_2	6950	98	295
3	PV-Cell	2330	148	677
4	$MAPbI_3$	1370	0.34	311
5	$MAPbBr_3$	3582	0.55	378
6	Rear Contact	2700	237	900

Table 3: Properties of materials used.

The properties in the table 3 are all required for the computational analysis. The electrical properties of the material are not considered for the simulation as it is beyond the scope of this paper. The analysis carried out in this study is only for the thermal analysis and hence the electrical property of these materials is not needed for this report.

The interaction of one layer with the other layer had to be within an acceptable realm so for that to happen an approriate boundary condition for the simulation had to be put. Boundary conditions in fluid dynamics are the set of constraints to the boundary value problem in computational fluid dynamics. These boundary conditions include inlet boundary conditions, outlet boundary conditions,

wall boundary conditions, constant pressure boundary conditions, axisymmetric boundary conditions, symmetric boundary conditions, and periodic or cyclic boundary conditions.

Tandem solar cell-1

The Table 4; describes the materials used in the tandem solar cell 1; where the uppermost layer is the glass. Then followed by the top sub cell material i.e. $MAPbI_3$. SnO_2 here is used as the intermediate layer between the two absorption layers. The bottom layer made up of mono crystalline Silicon; here described as PV-Cell. Lastly the rear contact layer made of aluminium. This tandem arrangement is kept, keeping in mind that mostly the Si is kept as the bottom sub cell. In most of the tandem arrangement the Si has lower band gap absorption capacity and the perovskite on the other hand have tuneable band gap (1.5-2.5 eV) which means their band gap energy absorption ability can be altered.

The tandem solar cell at present are mostly tried in combination with the perovskite. This is because of the versatility of perovskite. The tandem analysed here are all two junction tandem connected in series; tandem solar cell of more than two junctions are also possible like three junction and four junction; even in case of the multi junction tandem solar cell having more than two absorption layer the perovskite are used.

Sl. No.	*Name of the Material*	*Density (Kg/m^3)*	*Thermal Conductivity (W/m K)*	*Speccific Heat (J/ Kg K)*
1	Glass	3000	1.8	500
2	SnO_2	6950	98	295
3	PV-Cell(bottom)	2330	148	677
4	$MAPbI_3$(top)	1370	0.34	311
5	Rear Contact	2700	237	900

Table 4: Description of tandem solar cell 1.

Day 1 (16/05)					
		$MAPbI_3$		*PV-Cell*	
Sl.no.	*Time(Hr.)*	*Minimum Temperature(K)*	*Maximum Temperature(K)*	*Minimum Temperature(K)*	*Maximum Temperature(K)*
1	10:00	347	356	338	352
2	11:00	347	359	339	354
3	12:00	339	358	339	353
4	13:00	337	354	337	350
5	14:00	332	348	332	345
6	15:00	325	341	325	338
7	16:00	316	330	316	329
8	17:00	305	315	305	314

Table 5: Temperature recorded for the day 16/05 solar cell 1.

Day 2 (17/05)					
		$MAPbI_3$		*PV-Cell*	
Sl.no	*Time(Hr.)*	*Minimum Temperature(K)*	*Maximum Temperature(K)*	*Minimum Temperature(K)*	*Maximum Temperature(K)*
1	10:00	349	355	347	351
2	11:00	349	358	346	354

3	12:00	348	357	344	353
4	13:00	348	353	345	349
5	14:00	340	347	339	343
6	15:00	333	340	329	334
7	16:00	320	329	317	327
8	17:00	307	315	305	312

Table 6: Temperature recorded for the day 17/05 solar cell 1.

Day 3 (18/05)					
		$MAPbI_3$		*PV-Cell*	
Sl.no	*Time(Hr.)*	*Minimum Temperature(K)*	*Maximum Temperature(K)*	*Minimum Temperature(K)*	*Maximum Temperature(K)*
1	10:00	349	356	347	351
2	11:00	352	358	346	354
3	12:00	352	358	344	353
4	13:00	346	354	343	350
5	14:00	341	348	347	343
6	15:00	333	341	331	336
7	16:00	322	330	319	323
8	17:00	307	312	305	310

Table 7: Temperature recorded for the day 18/05 solar cell 1.

Day 4 (19/05)					
		$MAPbI_3$		*PV-Cell*	
Sl.no	*Time(Hr.)*	*Minimum Temperature(K)*	*Maximum Temperature(K)*	*Minimum Temperature(K)*	*Maximum Temperature(K)*
1	10:00	348	355	347	351
2	11:00	350	358	346	354
3	12:00	351	358	345	353
4	13:00	347	354	345	349
5	14:00	339	348	337	342
6	15:00	334	341	330	334
7	16:00	320	330	318	323
8	17:00	308	314	306	310

Table 8: Temperature recorded for the day 19/05 solar cell 1.

Day 5 (20/05)					
		$MAPbI_3$		*PV-Cell*	
Sl.no	*Time(Hr.)*	*Minimum Temperature(K)*	*Maximum Temperature(K)*	*Minimum Temperature(K)*	*Maximum Temperature(K)*
1	10:00	351	355	347	352
2	11:00	352	358	348	354
3	12:00	349	358	346	353

4	13:00	348	354	344	350
5	14:00	341	348	338	342
6	15:00	334	339	333	336
7	16:00	321	330	320	325
8	17:00	307	315	307	313

Table 9: Temperature recorded for the day 20/05 solar cell 1.

Day 6 (21/05)					
		$MAPbI_3$		***PV-Cell***	
Sl.no	***Time(Hr.)***	***Minimum Temperature(K)***	***Maximum Temperature(K)***	***Minimum Temperature(K)***	***Maximum Temperature(K)***
1	10:00	348	355	344	352
2	11:00	349	358	347	355
3	12:00	351	358	346	353
4	13:00	349	354	343	351
5	14:00	342	348	340	344
6	15:00	331	338	329	336
7	16:00	320	326	319	325
8	17:00	307	313	305	312

Table 10: Temperature Recorded for the day 21/05 solar cell 1.

Day 7 (22/05)					
		$MAPbI_3$		***PV-Cell***	
Sl.no	***Time(Hr.)***	***Minimum Temperature(K)***	***Maximum Temperature(K)***	***Minimum Temperature(K)***	***Maximum Temperature(K)***
1	10:00	348	355	346	351
2	11:00	351	358	346	354
3	12:00	351	358	346	353
4	13:00	346	354	344	350
5	14:00	340	348	338	342
6	15:00	333	341	330	338
7	16:00	321	330	318	328
8	17:00	308	315	306	313

Table 11: Temperature recorded for the day 22/05 of solar cell 1.

Tandem solar cell 2

Table12 comprises almost the same combination of materials with the exception of top sub cell or absorption layer i.e. $MAPbBr_3$ in this case. Rest the layers are in same arrangement. The thickness of this tandem solar cell is different as the layers included in this have been changed due to problem faced during meshing. The perovskite used here is kept as top absorption layer but as mentioned earlier ability of the perovskite to have tuneable band gap can make it possible for $MAPbBr_3$ to act as a bottom absorption layer. The thermo physical properties are only discussed here in this report. The electrical properties have been discussed in many reports prior to this but those properties are not necessary for the completion of this work as this report only focuses on the thermal aspect of the tandem solar cell.

Sl. No.	*Name of the Material*	*Density (Kg/m^3)*	*Thermal Conductivity (W/m K)*	*Specific Heat (J/ Kg K)*
1	Glass	3000	1.8	500
2	SnO_2	6950	98	295
3	PV-Cell(bottom)	2330	148	677
4	$MAPbBr_3$(top)	3582	0.55	378
5	Rear Contact	2700	237	900

Table 12: Description of tandem solar cell 2.

Day 1 (16/05)					
		$MAPbBr_3$		*PV-Cell*	
Sl. No.	*Time(Hr.)*	*Minimum Temperature(K)*	*Maximum Temperature(K)*	*Minimum Temperature(K)*	*Maximum Temperature(K)*
1	10:00	343	356	341	352
2	11:00	345	359	343	353
3	12:00	342	358	340	353
4	13:00	340	354	338	349
5	14:00	336	346	326	341
6	15:00	327	335	320	332
7	16:00	316	323	312	320
8	17:00	305	308	303	307

Table 13: Temperature recorded for day 16/05 of solar cell 2.

Day 2 (17/05)					
		$MAPbBr_3$		*PV-Cell*	
Sl. No.	*Time(Hr.)*	*Minimum Temperature(K)*	*Maximum Temperature(K)*	*Minimum Temperature(K)*	*Maximum Temperature(K)*
1	10:00	343	356	341	351
2	11:00	345	359	342	352
3	12:00	346	358	341	353
4	13:00	342	354	334	348
5	14:00	335	346	329	342
6	15:00	327	335	325	334
7	16:00	317	323	311	322
8	17:00	305	308	303	307

Table 14: Temperature recorded for the day 17/05 of solar cell 2.

Day 3 (18/05)					
		$MAPbBr_3$		*PV-Cell*	
Sl. No.	*Time(Hr.)*	*Minimum Temperature(K)*	*Maximum Temperature(K)*	*Minimum Temperature(K)*	*Maximum Temperature(K)*
1	10:00	343	356	342	351
2	11:00	348	359	344	353
3	12:00	349	358	343	352

4	13:00	343	354	341	350
5	14:00	336	346	330	342
6	15:00	328	335	326	334
7	16:00	318	323	315	322
8	17:00	306	309	301	304

Table 15: Temperature recorded for the day 18/05 of solar cell 2.

Day 4 (19/05)					
		$MAPbBr_3$		*PV-Cell*	
Sl. No.	*Time(Hr.)*	*Minimum Temperature(K)*	*Maximum Temperature(K)*	*Minimum Temperature(K)*	*Maximum Temperature(K)*
1	10:00	347	356	344	351
2	11:00	344	359	343	353
3	12:00	345	358	340	354
4	13:00	342	354	332	349
5	14:00	335	346	334	342
6	15:00	327	336	320	334
7	16:00	317	322	312	321
8	17:00	305	308	303	307

Table 16: Temperature recorded for the day 19/05 of solar cell 2.

Day 5 (20/05)					
		$MAPbBr_3$		*PV-Cell*	
Sl. No.	*Time(Hr.)*	*Minimum Temperature(K)*	*Maximum Temperature(K)*	*Minimum Temperature(K)*	*Maximum Temperature(K)*
1	10:00	345	356	338	352
2	11:00	347	359	339	352
3	12:00	340	358	337	354
4	13:00	340	354	336	350
5	14:00	335	346	329	343
6	15:00	326	336	322	334
7	16:00	317	323	312	322
Fig	Fig	306	308	305	308

Table 17: Temperature recorded for the day 20/05 of solar cell 2.

Day 6 (21/05)					
		$MAPbBr_3$		*PV-Cell*	
Sl. No.	*Time(Hr.)*	*Minimum Temperature(K)*	*Maximum Temperature(K)*	*Minimum Temperature(K)*	*Maximum Temperature(K)*
1	10:00	345	356	337	350
2	11:00	348	359	340	353
3	12:00	348	358	334	353
4	13:00	343	354	334	349

5	14:00	335	346	329	342
6	15:00	327	336	318	335
7	16:00	317	324	313	323
8	17:00	305	308	303	308

Table 18: Temperature Recorded for the day 21/05 of solar cell 2.

Day 7 (22/05)					
		$MAPbBr_3$		***PV-Cell***	
Sl. No.	***Time(Hr.)***	***Minimum Temperature(K)***	***Maximum Temperature(K)***	***Minimum Temperature(K)***	***Maximum Temperature(K)***
1	10:00	343	356	340	350
2	11:00	348	359	336	352
3	12:00	345	358	335	353
4	13:00	342	354	333	349
5	14:00	340	346	329	342
6	15:00	327	336	321	335
7	16:00	317	324	313	324
8	17:00	306	309	303	308

Table 19: Temperature recorded for the day 22/05 of solar cell 2.

Tandem solar cell-3

The tandem solar cell 3, composed of two perovskite as the absorption layer in both top and bottom sub cell. The rear contact is same as the other two tandem arrangement. The materials like the rear contact, glass have been kept with constant property as varying them could change the output of simulation drastically which wouldn't allow some common factors drawn among the three tandem arrangement. This combination of perovskite - perovskite can be arranged in two different ways of which only one type of the arrangement is used. As said earlier that a perovskite material has a tuneable band gap from 1.5- 2.5 eV this enables them to be easily used as any of the two sub-cells; the top absorption layer or the bottom absorption layer. Here in this report $MAPbBr_3$ is kept as the top layer and $MAPbI_3$ as the bottom layer as the result for this arrangement was better and within acceptable domain.

In the study, temperature difference between the two absorption layers were observed.

Sl. No.	***Name of the Material***	***Density (Kg/m^3)***	***Thermal Conductivity (W/m K)***	***Speccific Heat (J/ Kg K)***
1	Glass	3000	1.8	500
2	SnO_2	6950	98	295
3	$MAPbI_3$(bottom)	1370	0.34	311
4	$MAPbBr_3$(top)	3582	0.55	378
5	Rear Contact	2700	237	900

Table 20: Description of Tandem solar cell 3.

Day 1 (16/05)					
		$MAPbBr_3$		$MAPbI_3$	
Sl. No.	Time(Hr.)	Minimum Temperature(K)	Maximum Temperature(K)	Minimum Temperature(K)	Maximum Temperature(K)
1	10:00	333	356	330	352
2	11:00	343	359	334	354
3	12:00	345	358	334	354
4	13:00	342	354	329	350
5	14:00	335	346	325	344
6	15:00	327	335	322	334
7	16:00	316	323	311	322
8	17:00	305	308	303	307

Table 21: Temperature recorded for the day 16/05 of tandem solar cell 3.

Day 2 (17/05)					
		$MAPbBr_3$		$MAPbI_3$	
Sl. No.	Time(Hr.)	Minimum Temperature(K)	Maximum Temperature(K)	Minimum Temperature(K)	Maximum Temperature(K)
1	10:00	343	356	336	351
2	11:00	345	359	340	353
3	12:00	345	358	337	352
4	13:00	342	354	336	349
5	14:00	335	346	331	342
6	15:00	327	335	322	334
7	16:00	316	323	314	322
8	17:00	305	308	303	308

Table 22: Temperature recorded for the day 17/05 of tandem solar cell 3.

Day 3 (18/05)					
		$MAPbBr_3$		$MAPbI_3$	
Sl. No.	Time(Hr.)	Minimum Temperature(K)	Maximum Temperature(K)	Minimum Temperature(K)	Maximum Temperature(K)
1	10:00	343	356	341	351
2	11:00	346	359	336	353
3	12:00	348	358	339	353
4	13:00	341	354	334	347
5	14:00	335	346	330	342
6	15:00	327	335	322	334
7	16:00	317	323	316	322
8	17:00	305	308	303	308

Table 23: Temperature recorded for the day 18/05 of tandem solar cell 3.

Day 4 (19/05)					
		$MAPbBr_3$		$MAPbI_3$	
Sl. No.	Time(Hr.)	Minimum Temperature(K)	Maximum Temperature(K)	Minimum Temperature(K)	Maximum Temperature(K)
1	10:00	343	356	340	351
2	11:00	348	359	343	353
3	12:00	346	358	340	352
4	13:00	342	354	338	349
5	14:00	335	346	333	342
6	15:00	327	336	325	334
7	16:00	317	323	316	322
8	17:00	306	308	305	308

Table 24: Temperature recorded for the day 19/05 of tandem solar cell 3.

Day 5 (20/05)					
		$MAPbBr_3$		$MAPbI_3$	
Sl. No.	Time(Hr.)	Minimum Temperature(K)	Maximum Temperature(K)	Minimum Temperature(K)	Maximum Temperature(K)
1	10:00	347	356	342	352
2	11:00	345	359	342	353
3	12:00	348	358	342	353
4	13:00	342	354	337	349
5	14:00	337	346	332	340
6	15:00	327	336	324	334
7	16:00	317	323	313	322
8	17:00	305	308	304	307

Table 25: Temperature recorded for the day 20/05 of tandem solar cell 3.

Day 6 (21/05)					
		$MAPbBr_3$		$MAPbI_3$	
Sl. No.	Time(Hr.)	Minimum Temperature(K)	Maximum Temperature(K)	Minimum Temperature(K)	Maximum Temperature(K)
1	10:00	346	356	341	350
2	11:00	347	359	342	352
3	12:00	349	358	341	352
4	13:00	342	354	338	348
5	14:00	336	346	332	341
6	15:00	327	336	325	334
7	16:00	317	324	317	323
8	17:00	306	308	304	307

Table 26: Temperature recorded for the day 21/05 of tandem solar cell 3.

Day 7 (22/05)					
		$MAPbBr_3$		$MAPbI_3$	
Sl. No.	Time(Hr.)	Minimum Temperature(K)	Maximum Temperature(K)	Minimum Temperature(K)	Maximum Temperature(K)
1	10:00	347	356	342	351
2	11:00	344	359	341	352
3	12:00	345	358	347	356
4	13:00	344	354	340	348
5	14:00	345	346	336	342
6	15:00	327	336	325	335
7	16:00	316	324	314	323
8	17:00	306	309	305	307

Table 27: Temperature recorded for the day 22/05 of tandem solar cell 3.

Solar Flux Recorded

The value of solar flux displayed below is recorded for 7 days in the place Gangtok from 16/05-22/05. The unit of solar flux is W/m^2. The solar flux displayed is calculated using the solar calculator. The value of solar flux is same for all the tandem solar cells.

Sl. No.	Time (Hr.)	Date						
		16/05	17/05	18/05	19/05	20/05	21/05	22/05
1	10:00	903	901	900	899	897	896	895
2	11:00	912	910	909	908	906	905	904
3	12:00	910	908	907	906	905	903	903
4	13:00	897	895	894	893	892	891	890
5	14:00	869	868	867	865	864	863	863
6	15:00	816	815	814	813	812	811	811
7	16:00	713	712	712	711	711	710	710
8	17:00	469	470	470	473	475	476	478

Table 28: The hourly solar flux recorded during 7 days from 16/05 to 22/05.

Calculations

Calculation of average efficiency for a day

The average temperature of the solar cells at particular hour is to be calculated to find the efficiency of the solar cells as all that have been recorded are the maximum and minimum temperatures of the absorber at particular hour.

The average temperature can be calculated by using following relation:

$$Tavg = \frac{Tmax + Tmin}{2}$$

Where

T_{avg} = Average temperature of the cell. (°C)
T_{max} = Maximum temperature of the cell. (°C)
T_{min} = Minimum temperature of the cell. (°C)

After finding the average temperature of the cells the efficiency of the individual cell is calculated using the relation:

$$\eta_{ind} = 0.28 - 0.001 (T_{avg})$$

Where

η_{ind} = efficiency of the individual solar cell.
T_{avg} = average temperature of the cell. (°C)

Once the individual efficiency is calculated, the efficiency of the tandem has to be calculated. The efficiency

of the tandem is the sum of two individual layer's efficiency as:

$$\eta_{tandem} = \eta_{top} + \eta_{bottom}$$

Where:

η_{tandem} = efficiency of tandem.
η_{top} = efficiency of the top layer.
η_{bottom} = efficiency of the bottom layer.

Before using the above relations to find the efficiency of the solar cells with respect to their temperature, the temperature has to be converted to °C from K. Furthermore, the efficiency of Si layer is taken as 13.76% as stated earlier in model description section.

To display the calculation of each cell at each hour is not necessary as all the calculation is similar therefore calculation of only one solar cell for one day is displayed.

In this calculation the tandem solar cell 2 for the day 19/05 is selected.

The data is collected from Table 16.

Calculation for the top absorber layer of tandem solar cell 2 for the day 19/05 At 1000hr.

T_{max} = 356 K = 83°C
T_{min} = 347 K = 74°C

Therefore; Tavg = $\frac{83+74}{2}$ = 78.5°C

Now the efficiency of top layer i.e. $MAPbBr_3$ is

η_{ind} = 0.28 - 0.001 (78.5)

=0.2015

It can also be expressed as 20.15%.

Therefore, the efficiency of the tandem will be

$$\eta_{tandem} = \eta_{top} + \eta_{bottom}$$

$$\eta_{tandem} = 20.15+13.76 = 33.91$$

As the efficiency of the bottom cell is taken as constant.

Therefore, the efficiency of the tandem solar cell 2 at 10.00 hr. is 33.91%.

Similarly the average efficiency of a day for tandem solar cells for all cases considered is:

Day	*Tandem solar cell 1(%)*	*Tandem solar cell 2(%)*	*Tandem solar cell 3(%)*
16/05	35.25	35.35	43.78
17/05	35.01	35.31	43.55
18/05	34.94	35.24	43.52
19/05	34.96	35.38	43.38
20/05	34.93	35.33	43.38
21/05	35.01	35.25	43.36
22/05	34.95	35.24	43.22

Table 29: Average efficiency per day for tandem solar cell 1, 2 and 3.

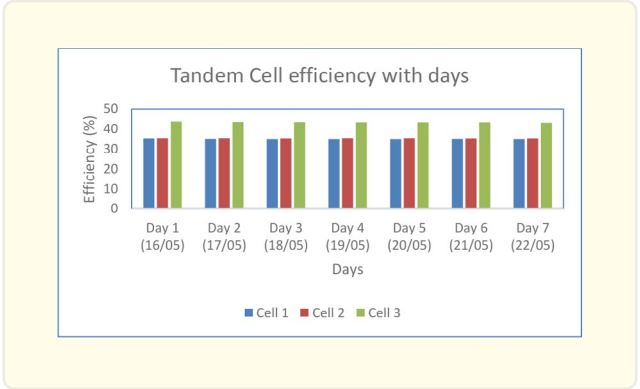

Calculation of average power converted per day

For this calculation we will consider the same tandem solar cell on the same day i.e. tandem solar cell 2 on 19/05.

To calculate the average power converted per day we need to have the value of incoming solar irradiation which can be taken from the table 28.

The value of incoming solar irradiance on 19/05 is:

Time	*10:00*	*11:00*	*12:00*	*13:00*	*14:00*	*15:00*	*16:00*	*17:00*
W/m^2	899	908	906	893	865	813	711	473

Table 30: Incoming solar flux for day 19/05.

The average incoming solar flux is = 808.5 W/m^2.

The average input power is calculated as

$$= \frac{incoming\ solar\ flux(\frac{W}{m^2})}{area\ of\ the\ solar\ cell(m^2)}$$

$$= \frac{808.5}{(2500 \times 10^{-3})^2}$$

$$= 129.36\ W$$

From table 29 efficiency of the tandem solar cell is 0.3538.

Therefore the energy converted =

$$efficiency \times average\ input\ power$$

= 0.3538*129.36 = 45.66 W

Day	*Tandem solar cell 1(W)*	*Tandem solar cell 2(W)*	*Tandem solar cell 3(W)*
Day 1 (16/05)	45.44	45.88	56.19
Day 2 (17/05)	45.08	45.76	55.79
Day 3 (18/05)	44.89	45.62	55.69
Day 4 (19/05)	44.91	45.66	55.47
Day 5 (20/05)	44.82	45.66	55.41
Day 6 (21/05)	44.87	45.51	55.33
Day 7 (22/05)	44.80	45.49	55.14

Table 31: Average output power given per day by tandem solar cells 1, 2 and 3.

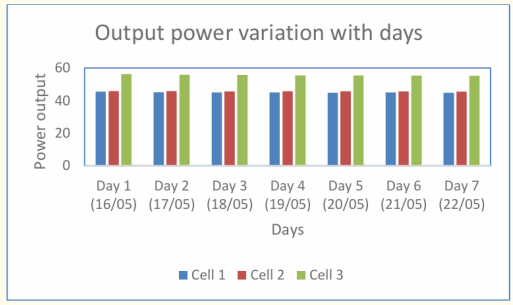

Results & Discussion

Results of Tandem Solar Cell-1

Result for the day 18/05

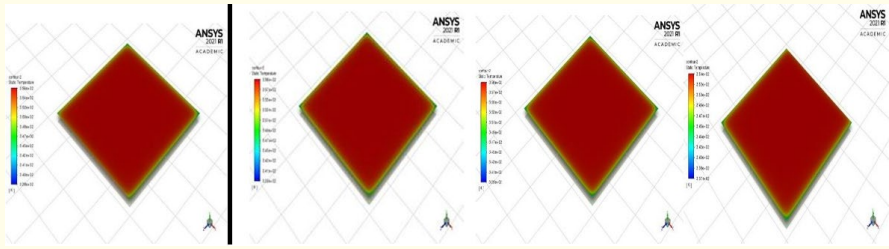

Figure 4: Temperature contour of top sub-cell from 1000hr. -1300hr.

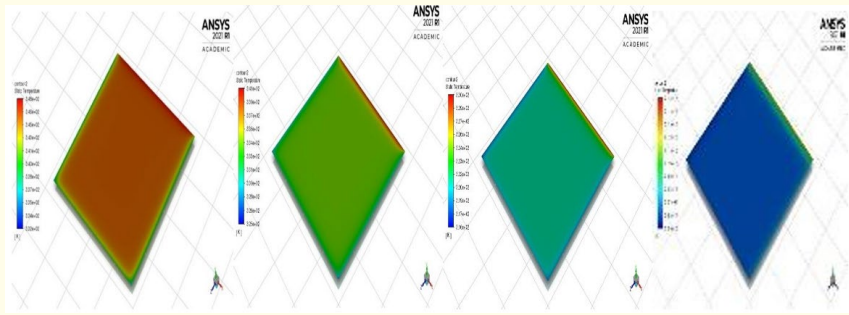

Figure 5: Temperature contour of top sub-cell from 1400hr. -1700hr.

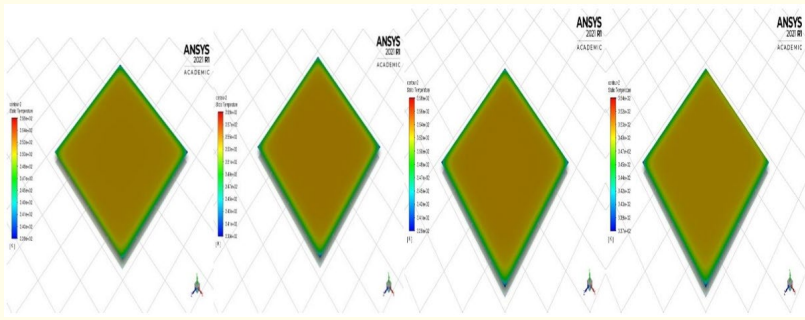

Figure 6: Temperature contour of bottom sub-cell from 1000hr. - 1300hr.

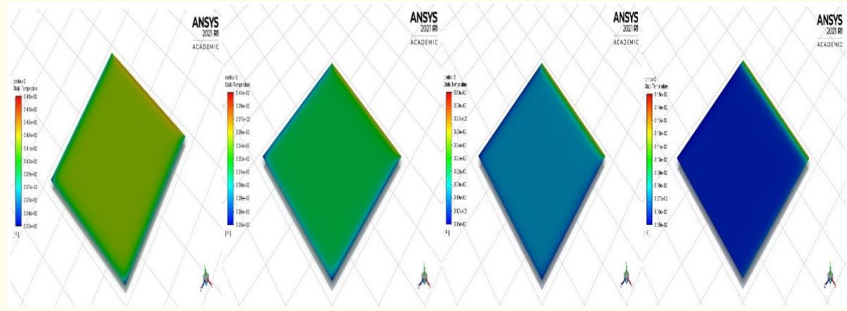

Figure 7: Temperature contour of bottom absorber from 1400hr. - 1700hr.

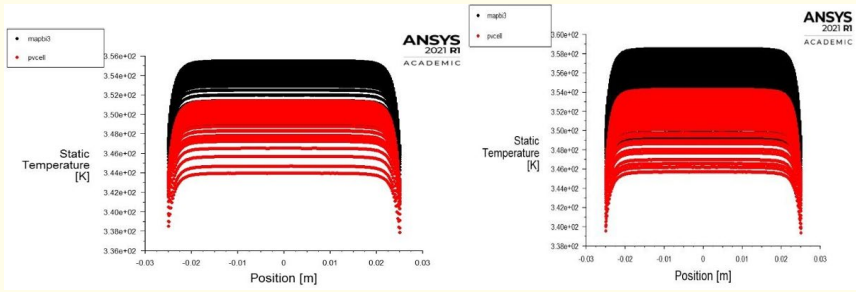

Figure 8: Temperature at 1000hr. ***Figure 9:*** Temperature at 1100 hr.

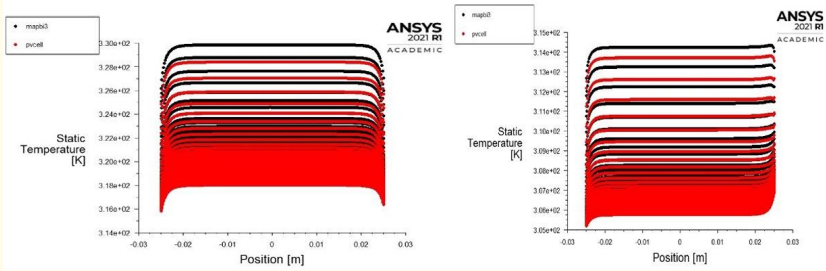

Figure 10: Temperature at 1600 hr. ***Figure 11:*** Temperature at 1700 hr.

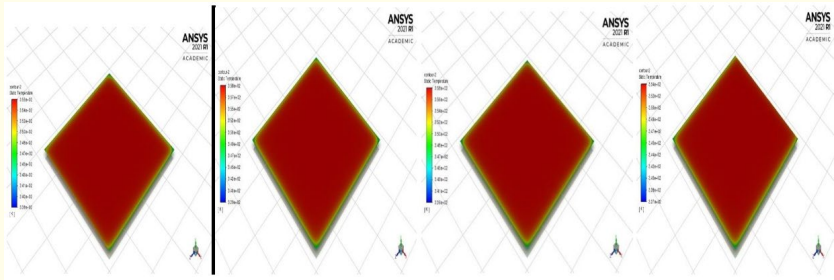

Figure 12: Temperature contour of top sub cell from 1000hr. -1300hr.

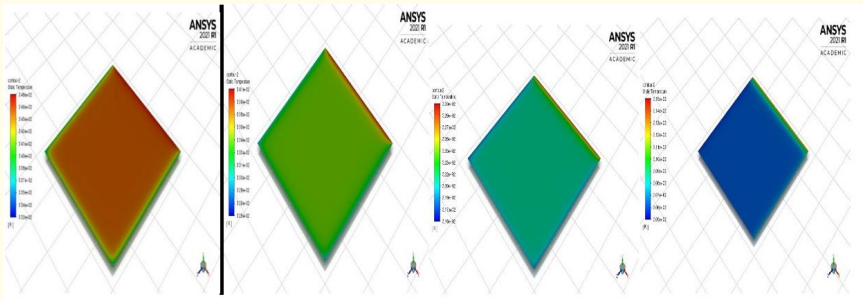

Figure 13: Temperature contour of top sub cell from 1400hr. -1700hr.

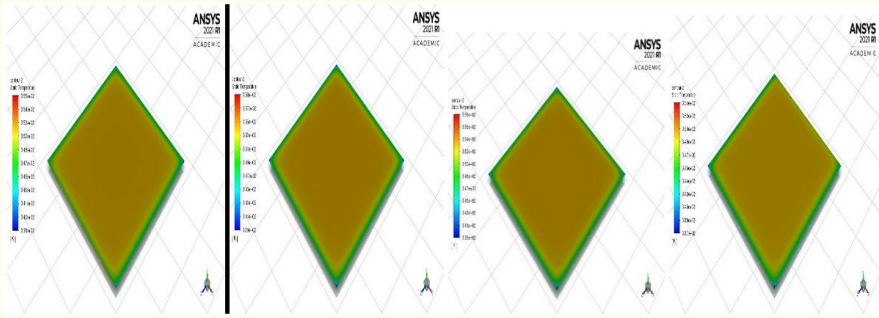

Figure 14: Temperature contour of bottom sub-cell from 1000hr. - 1300hr.

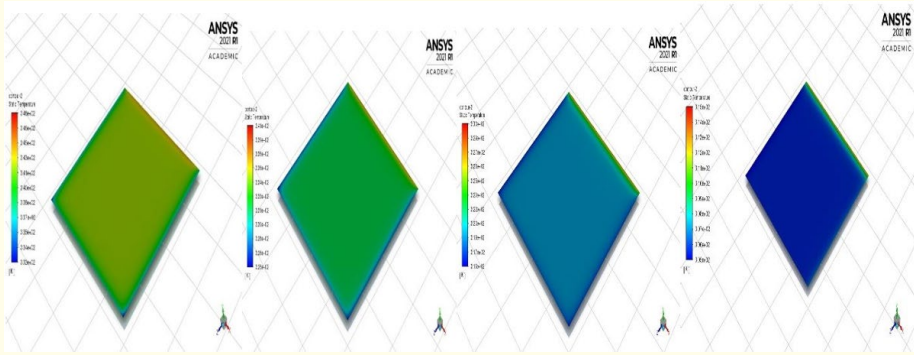

Figure 15: Temperature contour of bottom sub-cell from 1400hr. - 1700hr.

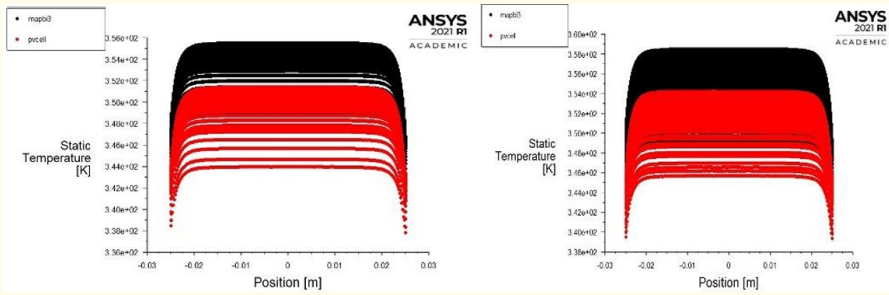

Figure 16: Temperature at 1000 hr. ***Figure 17:*** Temperature at 1100 hr.

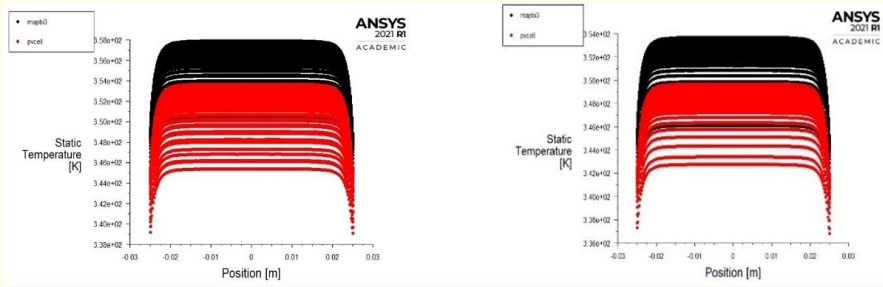

Figure 18: Temperature at 1200 hr. ***Figure 19:*** Temperature at 1300 hr.

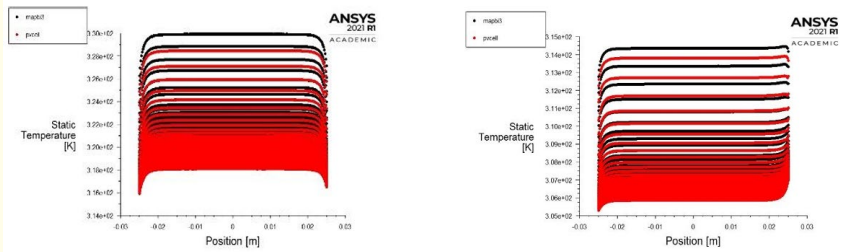

Figure 20: Temperature at 1600. ***Figure 21:*** Temperature at 1700.

Results of Tandem Solar Cell-2

Result for the day 16/05

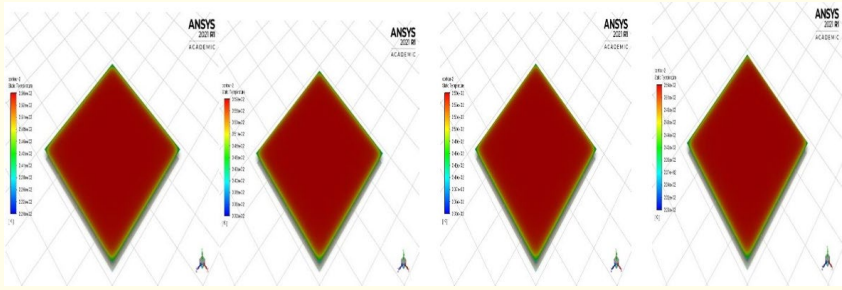

Figure 22: Temperature contour of top absorber layer from 1000hr. - 1300hr.

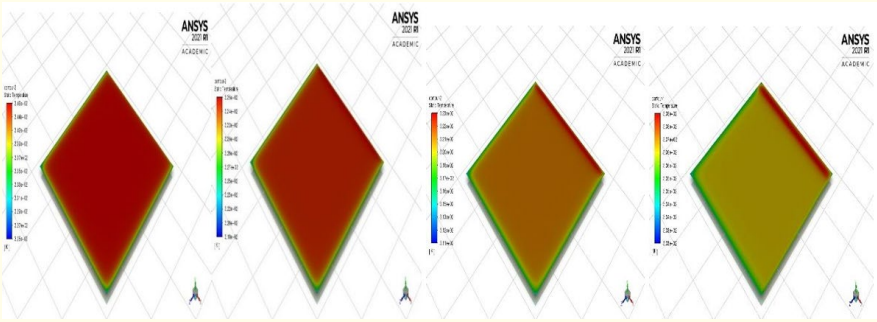

Figure 23: Temperature contour of top absorber layer from 1400hr. - 1700hr.

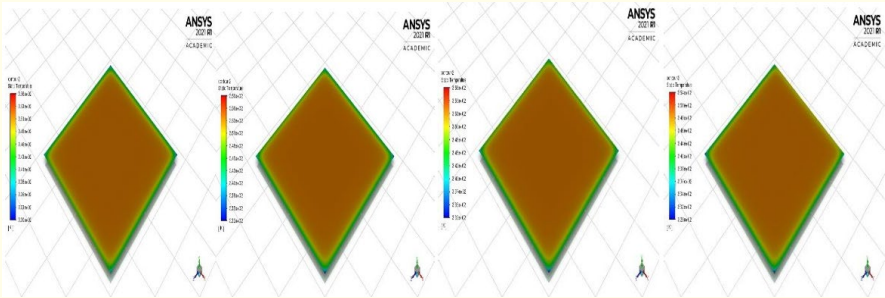

Figure 24: Temperature contour of bottom absorber layer from 1000hr. - 1300hr.

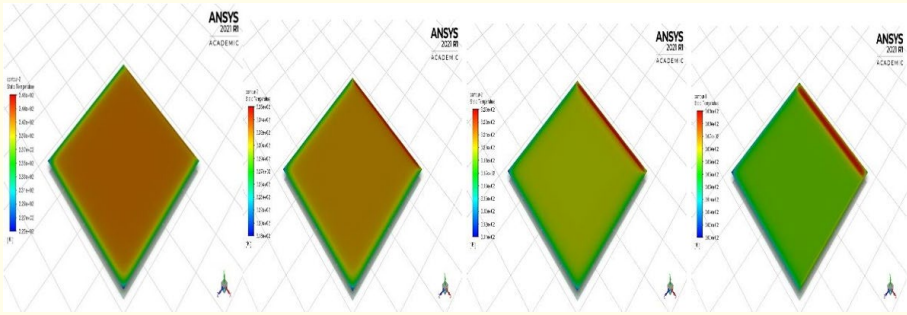

Figure 25: Temperature contour of bottom absorber layer from 1400hr. - 1700hr.

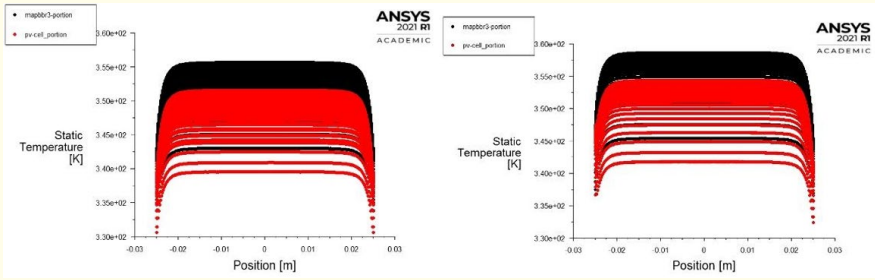

Figure 26: Temperature at 1000hr. ***Figure 27:*** Temperature at 1100 hr.

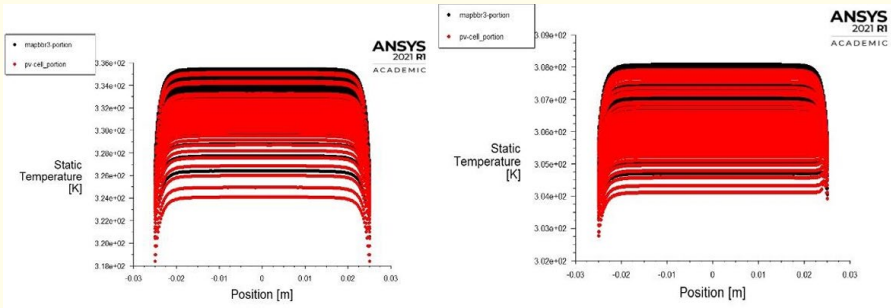

Figure 28: Temperature at 1500 hr. ***Figure 29:*** Temperature at 1700hr.

Results of Tandem Solar Cell-3

Result for the day 22/05

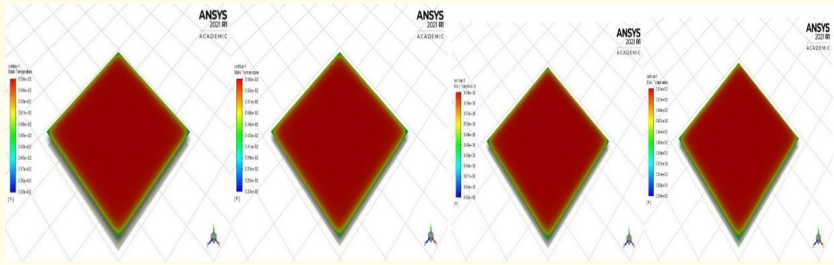

Figure 30: Temperature of the top sub-cell from 1000hr. -1300hr.

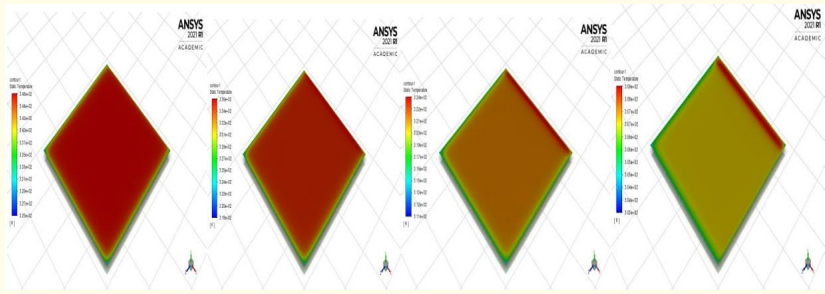

Figure 31: Temperature of the top sub-cell from 1400hr. -1700hr.

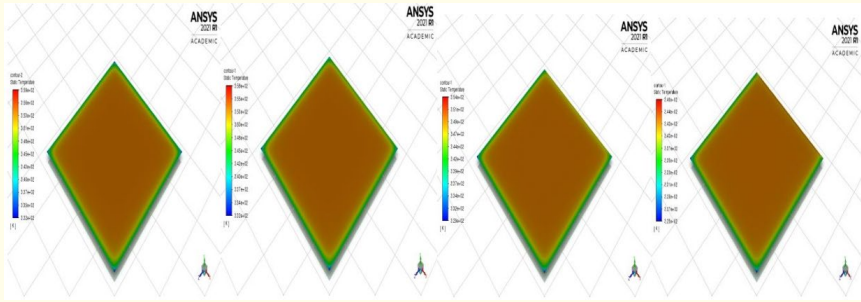

Figure 32: Temperature contour of the bottom cell from 1100hr. - 1400hr.

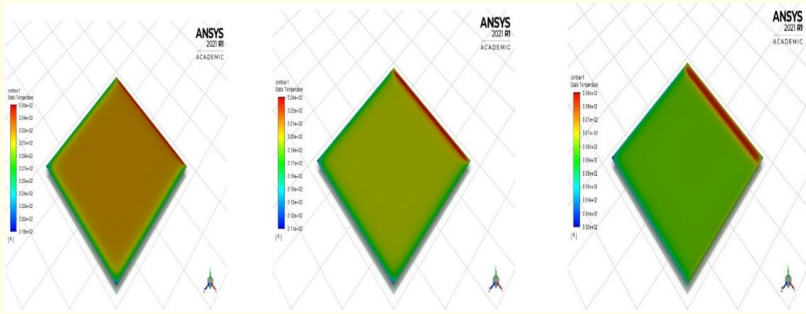

Figure 33: Temperature contour of the bottom cell from 1500hr. - 1700hr.

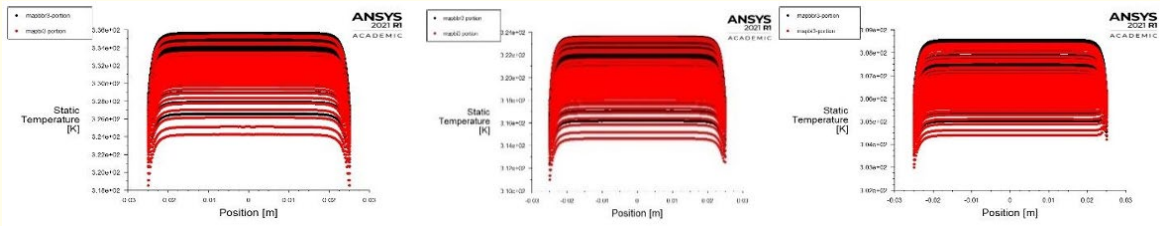

Figure 34: Temperature at 1500 hr. ***Figure 35:*** Temperature at 1600 hr. ***Figure 36:*** Temperature at 1700 hr.

The temperature plots for different tandem cells have been compared for the whole day hourly basis starting from 10.00 AM to 5.00 PM for a week. From the temperature contour plot it has been observed that the temperature increases from 10.00 AM to 11.00 AM and then gradually decreases towards 5.00 PM. The variation of temperature is different for different solar tandem cells. As compared to $MAPbI_3$ tandem the $MAPbBr_3$ cell is achieving more temperature from 11.00 AM up to 1.00 PM and then gradually decreases.

Conclusions

The thermal analysis of the three tandem solar cells for the place Gangtok is done computationally and the results are displayed. The tandem solar cells in this place have shown in this study that the maximum temperature it can reach is about 360 K which is about 87°C. The efficiency calculated for the tandem solar cells are displayed in table 29. The efficiency calculated is the efficiency of a particular tandem solar cell on particular day i.e. from 16/05- 22/05.

The average output power for each tandem solar cell for 7 days from 16/05 to 22/05 is presented on the table 30 wherein the output power generated by tandem as a whole is displayed. The output power and the efficiency that are calculated in the paper are purely based on the temperature of the absorber layer.

The result displayed is from 16-22 May which is a time in a year at which the place experiences high average temperature as well as maximum solar irradiation and also the day time is longest. As the efficiency calculated is in terms of temperature therefore the day is chosen so as the temperature of the cells will probably be highest at this time of year.

The solar irradiance of this place is shown to maximum at 11.00 hr. which is not applicable for other places of India as in plain areas the maximum solar irradiance is at around 12.30-13.30. hr. the trend in the efficiency in terms of temperature for this place increases from 14.00 hr. because the solar irradiance is high and the temperature is low as compared to the other time of the day where the irradiation as well as temperature is high.

In most of the results displayed in the paper the temperature of the top and bottom absorber layer differs greatly in their earlier hours of the day whereas the difference is minimized as the hour passes this is because the solar cell's mesh orientation is constant and so the solar ray incident on the cells tends to be from the side which affects the temperature of the sub-cells and rises their temperature to nearly similar value. All this can be viewed and confirmed from the temperature contours of different tandem solar cells and also through the X-Y plot of the temperature for two sub-cells on hourly basis.

The efficiency reported in the study can have different values as it usually happens when we do recording on real life situations due to many factors; as the place experiences a lot of overcast weather that can drastically alter the actual solar irradiation in the place. The simulation was for the condition of fair weather; because the place experiences a lot of rainfall at this time of year actual value of incoming power may vary. The temperature recorded for this paper is theoritical in all sense as the wind is not considered and it could help in lowering the temperature of the solar cell. The place experiences a lot of cool winds that are on average 5-6 Km/hr.; which can act as cooler for the solar panel that drops the temperature and changes the overall efficiency of the system.

References

1. T Todorov, AO Gunawana and S Guha. Article in Molecular Systems Design & Engineering A road towards 25% efficiency and beyond: perovskite tandem solar cells (2016).
2. Cătălin George Popovicia., et al. Sustainable Solutions for Energy and Environment, EENVIRO - YRC 2015, Bucharest, Romania; Efficiency improvement of photovoltaic panels by using air cooled heat sinks (2015).
3. Fangyuan Jiang., et al. "A two- terminal perovskite/perovskite tandem solar cell". Journal of Materials Chemistry A (2015).
4. Mihai Răzvan Mitroi, Valerică Ninulescu and Laurenţiu Fara. "Tandem Solar Cells Based on Cu_2O and c-Si Subcells in Parallel Configuration: Numerical Simulation". International Journal of Photoenergy (2017): 7284367.
5. Monjur Mourshed., et al. "Experimental investigation and CFD analysis of a solar hybrid PV/T system for the sustainable development of the rural northern part of Bangladesh". International Journal of Sustainable Energy (2018).
6. Hiren D Raval, Subarna Maiti and Ashish Mittal. "Computational fluid dynamics analysis and experimental validation of improvement in overall energy efficiency of a solar photovoltaic panel by thermal energy recovery". Journal of Renewable and Sustainable Energy (2014): 033138.
7. Ashish Saurabh, Deepali Atheaya and Anil Kumar. Department of Mechanical and Aerospace Engineering, Bennett University, Tech Zone - II, Greater Noida, 201310, UP, India.
8. M Sabry. "Temperature optimization of high concentrated active cooled solar cells". NRIAG Journal of Astronomy and Geophysics 5.1 (2016): 23-29.
9. Malagouda Patil, Dr. Alur Sidramappa, Rajashekhar. Goud Angadi Experimental Investigation of Enhancing the Energy Conversion Efficiency of Solar PV Cell by Water Cooling Mechanism.
10. Kudzanayi Chiteka, Rajesh Arora and Vineet Jain. "CFD prediction of dust deposition and installation parametric optimisation for fouling mitigation in non-tracking solar PV modules". International Journal of Ambient Energy (2019).
11. AN Özakın., et al. "The heat recovery with heat transfer methods from solar photovoltaic systems". International Physics Conference at the Anatolian Peak (IPCAP2016) IOP Publishing Journal of Physics: Conference Series 707 (2016): 012050.

12. Teodor K Todorov, Douglas M Bishop and Yun Seog Lee. "Materials perspectives for next-generation low-cost tandem solar cells". Solar Energy Materials and Solar Cells (2017).
13. Gökhan Ömeroğlu. "CFD Analysis and Electrical Efficiency Improvement of a Hybrid PV/T Panel Cooled by Forced Air Circulation". International Journal of Photoenergy (2018): 9139683.
14. Ruijun Zhang, Yangyu Gan and Parham A Mirzaei. "A new regression model to predict BIPV cell temperature for various climates using a high resolution CFD microclimate model". Advances in Building Energy Research (2019).
15. Fan Fu., et al. "Low-temperature-processed efficient semi-transparent planar perovskite solar cells for bifacial and tandem applications". Nature Communications 6 (2015): 8932.
16. Jaemin Kim., et al. "Experimental and Numerical Study on the Cooling Performance of Fins and Metal Mesh Attached on a Photovoltaic Module". Energies 13.1 (2020): 85.
17. Toru Ashida., et al. "Thermal transport properties of polycrystalline tin-doped indium oxide films". Citation: J. Appl. Phys 105 (2009): 073709.
18. Tobias Haeger, Ralf Heiderhoff and Thomas Riedl. "Thermal properties of metal-halide perovskites". Journal of Materials Chemistry C 41 (2020).

Volume 7 Issue 4 October 2024